Lab on a Chip

Spatial tuning of acoustofluidic pressure nodes by altering net sonic velocity enables high-throughput, efficient cell sorting

Journal:	*Lab on a Chip*
Manuscript ID:	LC-TIN-11-2014-001342.R1
Article Type:	Technical Innovation
Date Submitted by the Author:	20-Dec-2014

Complete List of Authors:	Jung, Seung-Yong; University of California, San Francisco, Biochemistry and Biophysics Notton, Timothy; University of California, San Francisco, Biochemistry and Biophysics; UC, Berkely and UC, San Francisco, Joint Graduate Group in Bioengineering Fong, Erika; Lawrence Livermore National Laboratory, Materials Engineering Division; Boston University, Biomedical Engineering Shusteff, Maxim; Lawrence Livermore National Laboratory, Weinberger, Leor; University of California, San Francisco, Biochemistry and Biophysics

SCHOLARONE™
Manuscripts

Cite this: DOI: 10.1039/c0xx00000x

www.rsc.org/xxxxxx

Technical Innovations

Spatial tuning of acoustofluidic pressure nodes by altering net sonic velocity enables high-throughput, efficient cell sorting

Seung-Yong Jung,[a,b] Timothy Notton,[a,c] Erika Fong,[d,e] Maxim Shusteff*[d] and Leor S. Weinberger*[a,b,f]

Received (in XXX, XXX) Xth XXXXXXXXX 20XX, Accepted Xth XXXXXXXXX 20XX

DOI: 10.1039/b000000x

Particle sorting using acoustofluidics has enormous potential but widespread adoption has been limited by complex device designs and low throughput. Here, we report high throughput separation of particles and T lymphocytes (600 µL/min) by altering the net sonic velocity to reposition acoustic pressure nodes in a simple two-channel device. The approach is generalizable to other microfluidic platforms for rapid, high-throughput analysis.

Biological fluids, particularly clinical samples, are complex, inherently heterogeneous mixtures that contain particles with highly variant shapes and sizes. Precise analysis of the constituent particles from these fluids often requires separation and enrichment of the specific target particles from this complex mixture. When these targets exist at low concentrations, such as in the early stages of disease, high-throughput approaches (that are biocompatible) are necessary. One attractive approach is acoustophoresis—manipulating suspended analyte particles with ultrasonic standing waves. This gentle (i.e. contactless) and label-free approach sorts particles based on their physical properties, such as size, density, and compressibility[1,2]. Acoustophoresis has been adapted for a wide range of applications that require well-controlled conditions provided by laminar flow, such as sorting or synchronizing cells[3], manipulating single cells[4], enriching circulating tumor cells[5], and separating cells from virus[6].

In acoustophoresis, particle separation occurs due to acoustic radiation forces that arise from an acoustic sound–pressure field acting upon particles suspended in fluid[7]. These forces are proportional to particle volume, making particle size the most accessible separation parameter. When the acoustic contrast factor, a number depending on a particle's density and compressibility in relation to the suspending fluid, is positive, which is the case in most applications, the forces transport particles toward the pressure minima (nodes) of the standing wave, with larger particles moving rapidly, while smaller particles or dissolved species remain on their original laminar streamlines.

In microfluidic separation applications, an ultrasonic standing wave can be generated by attaching a piezoelectric actuator to the back of a silicon etched channel structure. The piezo driving frequency can then be tuned to match the width or height of the microfluidic channel. These dimensions set the harmonic

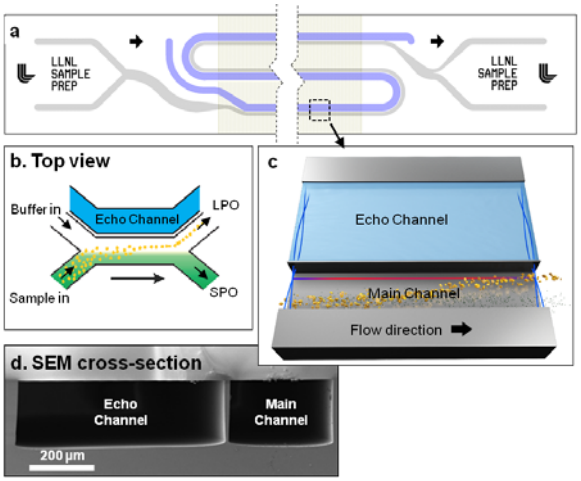

Figure 1. The dual-channel acoustofluidic device. (a) Top-view of the photomask layout used to etch silicon channels. The separation channel is shaded gray and the echo channel blue. The chip center section (with straight channels) is cut away for compactness. Overall chip dimensions are 70 mm long x 9 mm wide. The piezoceramic acoustic-force generating transducer (37 mm long x 9 mm wide) is bonded to the underside of the slide, with the fluid channel making three passes through the piezo region. (b) Simplified schematic of fluid flows and channel inlets and outlets (acoustic force generator is on the underside). (c) Rendering of the decoupled fluidic and acoustic geometries (the fluid that fills the main channel is omitted for clarity). The silicon wall separating the channels is transparent to ultrasound, producing a continuous field of sound pressure (blue curves at edges) across both channels. The red line indicates the position of the pressure focus node in the main channel, and the larger particles (yellow cells) migrate to the node as they flow through the device. (d) SEM image of the dual-channel cross-section showing the silicon wall. Scale bar = 200 µm.

resonance modes in the fluid, which predict the number and positions of nodal planes. The most common mode is the half-wave resonance, with the nodal plane at the center of the channel. However, these pre-determined and symmetric nodal positions are not easily adjustable, which limits the flexibility of the device. For example, modulating only the axial distance from the input streamline to the focal position could be insufficient to achieve the required throughput for samples where volumes of several milliliters must be rapidly processed. Other studies examined acoustophoretic devices with asymmetric or adjustable locations for nodal planes[8-12] and while these devices are exceptionally elegant and exhibit impressive separation efficiency, unfortunately, they are limited by low sample throughput, with

separation channel flow rates limited to ≤ 10 µL/min.

Here, we present an approach to maintain total flow rates over 200 µL/min while allowing adjustable node positioning. We utilize our previously reported device[6], with a two-channel geometry comprising a main sample separation channel and a secondary "bypass" (or "echo") channel separated from the main channel by a thin silicon wall. These parallel channels run adjacent to each other, and interact acoustically, but not fluidically (Fig. 1). Channels are anisotropically deep reactive–ion etched 200 µm deep on <100> silicon wafers[6]; the widths of the main and echo/bypass channels are 300 and 597 µm, respectively, and they are separated by a thin 10 µm silicon wall. After anodically bonding borosilicate glass to seal the channel, this wall creates a physical barrier that prevents media from mixing between different channels, but allows ultrasonic waves to pass through. By driving the second harmonic resonant-mode, two pressure nodes spanning both channels are generated (Fig. 1C). Thus, the device allows the acoustic focus to be positioned asymmetrically in the main channel (when both channels were filled with the same fluid[6]). The sample co-flows with a clean buffer stream in the main channel, which has two inlets and two outlets. When the acoustic field is off, all particles remain on their original streamlines, and exit from the small particle outlet (SPO). With the field on, however, large particles are separated from their initial streamlines toward the pressure node, exiting from the large particle outlet (LPO).

To explore the possibility of decoupling the spatial location of the acoustic pressure nodes from the physical geometry of the device, we examined the effect of filling the echo channel with media other than water, having different bulk elastic moduli and densities, and, therefore, different speeds of sound. Specifically, we test if these different media result in fine-tuning of the resonance frequency and the focusing position in the main channel. The position of the acoustic focus in the main separation channel can be spatially adjusted by changing the speed of sound in the echo channel, using fluids that exhibit different ultrasonic velocities. By considering the speeds of sound within the bypass fluid and silicon, the resonant structure can be analyzed as having an effective "water-equivalent" width (W_{eff}). This effective width is used to estimate the focal position in the main channel and is defined as the distance that ultrasonic waves would travel if all regions were water (both echo and main channels, as well as the silicon wall). This is calculated by scaling each region by its relative speed of sound compared to water as follows:

$$W_{eff} = W_{main} + W_{echo}\,(C_w/C_{echo}) + W_{wall}\,(C_w/C_{si})$$

where W_{main} is the width of the main channel (300 µm) that is always filled with water, W_{echo} is the width of the echo channel (597 µm), W_{wall} is the thickness of the Si barrier (10 µm), and C_w, C_{si}, and C_{echo} indicate the speed of sound in water, Si, and the bypass fluid, respectively.

Importantly, reliable operation of the acoustophoretic device requires temperature stability during experiments, since temperature changes affect the speed of sound. Along with an external cooling fan, the bypass fluid is cooled in an ice bath and circulated through the chip at 1 mL/min with a peristaltic pump (VWR, Radnor, PA). Thus, the echo channel also serves as a heat sink to maintain the temperature of the entire chip (monitored by an attached thermocouple) at 26°C, with fluctuations of only ±1°C at operating voltages.

To demonstrate that the focusing position in these devices can be shifted in either direction, we tested three fluids in the echo channel that provide a range of sound speeds[13,14]: 50% (mole fraction) glycerol in water (higher glycerol content is too viscous to be practical); 50% (mole fraction) ethanol in water; and 100% ethanol. The C_{echo} values of these fluids are summarized in Fig. 2. The expected resonance frequency (f_0) with each fluid is calculated from W_{eff} by $f_0 = nC_w/2W_{eff}$, where n is the number of pressure nodes (n = 2 for this device). To observe the acoustic focusing performance at the resonance frequency, we imaged 10.2 µm diameter fluorescent polymer microspheres (0.01% w/v in 1X PBS, Spherotech, Inc., Lake Forest, IL, USA) co-flowing with clean PBS at a total flow rate of 800 µL/min in the main channel (400 µL/min per inlet). For all experiments (including cell separation described below) LPO and SPO flow rates were monitored by flow meters (Sensirion AG, Switzerland), and flow was split passively at the outlets, and collected in vials.

To find the resonant frequencies f_0 with each medium, we scanned the driving frequencies of the transducer in steps of 0.02 MHz between 1.30 and 2.00 MHz and an operating voltage of 15 V, and identified f_0 as the frequency at which the full width at half maximum (FWHM) from fluorescence intensity profiles is minimized. The measured impedance was 15 - 20 ohms in the

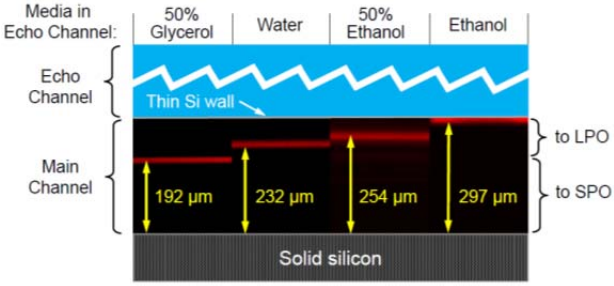

Media	50% Glycerol	Water	50% Ethanol	100% Ethanol
Distance measured (calculated), µm	192 (192)	232 (225)	254 (240)	297 (270)
Resonance Frequency measured (calculated), MHz	1.80 (1.93)	1.62 (1.65)	1.43 (1.55)	1.34 (1.38)

Figure 2. Focus positions in the separation channel with different fluids in the echo channel. Different focus positions in the main separation channel were observed with a suspension of 10.2 µm fluorescent polystyrene beads (0.01% w/v) at a total flow rate of 800 µL/min. Red lines indicate position of the focused beads in the presence of different fluids in the echo channel. To find each resonance frequency, the piezo actuator drive was scanned at intervals of 0.02 MHz between 1.30 and 2.00 MHz at an actuation voltage of 15 Vpp. The table indicates experimental values compared with 1-D model calculations.

This journal is © The Royal Society of Chemistry [year]

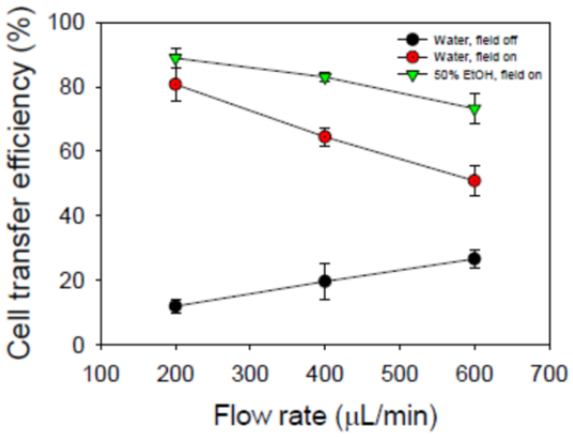

Figure 3. Cell transfer efficiency of MT-4 lymphocytes stained with CellTracker™ Red CMTPX dye at a range of total main-channel flow rates with different fluids in the echo channel. Cells were counted by flow cytometry. Transfer efficiency was calculated as the percentage of cells collected from the LPO among the total number of cells collected from both outlets. Black dots indicate cell transfer efficiencies without applying the acoustic force. Red dots and green inverted triangles represent the acoustic cell transfer efficiencies with water and 50% ethanol in the echo channel in presence of acoustic driving force values in table in Fig. 2., respectively.

relevant frequency range and resulting maximum dissipated power was 5.5 – 7.5 W for 15 Vpp drive. The calculated and measured resonant frequencies for each fluid combination are indicated in Fig. 2. 50 % ethanol moved the focal position by 22 μm toward large particle outlet (LPO) compared to water, while the focal position with 100% ethanol was shifted by 65 μm compared to water. In contrast, 50% glycerol, in which sound travels faster, moved the focal position 40 μm in the opposite direction (toward the center of the main channel). A key result of these experiments is that a 50% aqueous ethanol solution provides the optimal fluid for the echo channel. With 100% ethanol, the pressure node approaches too close to the dividing wall, where the downstream velocity of the fluid streamlines is close to zero. This caused particle aggregation at the focusing position at multiple locations along the wall, thereby blocking the channel (data not shown). Overall, these results show that microparticle trajectories can be manipulated over a range of 100 μm across the main channel by altering the fluid in the echo channel.

Finally, to test if this approach could be used for live-cell separation, we pumped human MT-4 T lymphocytes suspended in growth media (RPMI 1640 with 10% FBS, Corning Cellgro, Manassas, MA) through the main channel, co-flowing with clean RPMI media, at total flow rates of 200, 400, and 600 μL/min (average flow speeds of 55, 110, and 165 mm/s, and estimated Reynolds numbers of 15, 30, and 45, respectively), and then compared the separation efficiency with either water or 50% ethanol in the echo channel. Cells were visualized by staining with CellTracker™ Red CMTPX Dye (Molecular Probes), collected at both chip outlets, and cell numbers were analyzed on a MACSQuant® VYB flow cytometer (Miltenyi Biotec GmbH, Bergisch Gladbach, Germany). Cell-transfer efficiency was calculated as the percentage of cells exiting the large particle outlet (LPO) compared with the total number of cells exiting the device. In the absence of the acoustophoretic force field, 73-88% of cells remained in the original flow stream and exited from the SPO. Some movement of cells out of the SPO is attributable to the "switchbacks" in the geometry of the microfluidic chip, which provide more residence time for particles to experience acoustic forces, but also induce Dean flow at the two turns. These Dean vortices spill some cells into the LPO, which becomes more pronounced with increasing flow rate and Reynolds number. Nevertheless, even at 600 μL/min, the majority of cells remain on their original laminar streamlines and exit from the SPO (Fig. 3, black dots). When the acoustic field is activated at relatively low flow velocities (200 μL/min), the efficiencies with pure water (red dots) and 50% ethanol (green inverted triangles) in the echo channel are 81% and 89%, respectively. However, at 600 μL/min, the separation efficiencies are significantly different (51% cell-transfer efficiency with water in the echo channel and 73% cell-transfer efficiency with 50% ethanol). Also, it should be mentioned that this separation efficiency was achieved with the simple single transducer while dual piezo system and pre-alignment were required in the previous report by Laurell group[5] to demonstrate impressive separation efficiency (over 90% with 560 μL/min). The possible integration of pre-alignment into this echo channel system would give even better separation. When switching from water to 50% ethanol in the echo channel, the pressure node position moves from 232 μm (distance from the solid silicon wall) to 254 μm. These findings indicate that placing ethanol in the echo channel improves separation, likely because the focusing position is closer to the LPO, and the linear velocity at this position is slower. The linear velocity of the streamline at the 232 μm position is about 20% faster than that at 254 μm (COMSOL simulation, data not shown) because of the characteristic parabolic profile of pressure-driven Poiseuille flow. Intuitively, the slower linear velocity of particles induced by 50% ethanol in the echo channel increases cells' exposure to the standing acoustic waves and thus improves focusing, especially at high-flow rates.

Conclusions

In summary, this report describes a new method to precisely control the nodal position in an acoustofluidic device by exploiting differences in specific gravity and ultrasonic velocities without changing the physical dimensions of channels, which typically requires new fabrication. By changing the media composition in an adjacent echo channel, the pressure node can be dynamically repositioned transverse to the flow direction. Based on this method, extremely high-throughput (an order of magnitude faster flow rates than previous adjustable-node acoustofluidic designs) and highly-selective separation of particles can be obtained by tuning the nodal band closer to the desired outlet. This novel approach relaxes some of the strict geometric constraints of acoustophoretic designs for microfluidic chips. It may also promote more flexibility in exploring challenging applications, such as developing simple and automated binary valves, building cell sorters with multiple and lateral outlets, or integrating with other microfluidic systems.

Acknowledgements

The authors thank J. Hamilton and E. Behymer (LLNL Microtechnology Center) for device fabrication and K. Chu for the 3-D graphics. This work was supported by the NIH Director's Pioneer Award Program award OD017181 (L.S.W.), NIH award AI109611 (L.S.W.), and by the UC Office of the President Lab Fees Research Program, Grant ID #237909 (L.S.W.). M.S. acknowledges support from the U.S. Department of Energy (DE-AC52-07NA27344), and the LLNL LDRD program (14-LW-077). EJF acknowledges support from the LLNL Lawrence Scholar Graduate Program. LLNL-JRNL- 665514.

Notes and references

[a] *Department of Biochemistry and Biophysics, University of California, San Francisco, CA 94143, USA. Fax: 415- 355-0855; Tel: 415-734-4857; E-mail: leor.weinberger@gladstone.ucsf.edu*
[b] *Gladstone Institutes, 1650 Owens Street, San Francisco, CA 94158, USA.*
[c] *Joint Graduate Group in Bioengineering, University of California, Berkeley and University of California, San Francisco, CA 94158, USA.*
[d] *Lawrence Livermore National Laboratory, Livermore, CA 94550, USA. E-mail: shusteff1@llnl.gov*
[e] *Department of Biomedical Engineering, Boston University, Boston, MA 02215, USA.*
[f] *QB3: California Institute for Quantitative Biosciences, University of California, San Francisco, CA 94158, USA.*

1 T. Leong, L. Johansson, P. Juliano, S. L. McArthur, R. Manasseh, *Ind. Eng. Chem. Res.,* 2013, **52,** 16555–16576.
2 A. Lenshof, C. Magnusson, T. Laurell, *Lab Chip*, 2012, **12,** 1210–1223.
3 A. H. Yang, H. T. Soh, *Anal. Chem.,* 2012, **84,** 10756–10762.
4 X. Ding, S. C. Lin, B. Kiraly, H. Yue, S. Li, I. K. Chiang, J. Shi, S. J. Benkovic, T. J. Huang, *PNAS*, 2012, **109,** 11105–11109.
5 P. Augustsson, C. Magnusson, M. Nordin, H. Lilja, T. Laurell, *Anal. Chem.*, 2012, **84,** 7954–7962.
6 E. J. Fong, A. C. Johnston, T. Notton, S. Y. Jung, K. A. Rose, L. S. Weinberger, M. Shusteff, *Analyst*, 2014, **139,**1192–1200.
7 H. Bruus, *Lab Chip*., 2012, **12,** 1014-21.
8 S. Kapishnikov, V. Kantsler, V. Steinberg, *J. Stat. Mech.*, 2006, P01012.
9 P. Glynne-Jones, R. J. Boltryk, N. R. Harris, A.W. Cranny, M. Hill, *Ultrasonics,* 2010, **50,** 68-75.
10 L. Meng, F. Cai, Z. Zhang, L. Niu, Q. Jin, F. Yan, J. Wu, Z. Wang, H. Zheng, *Biomicrofluidics,* 2011, **5,** 44104-4410410.
11 N. D. Orloff et al., *Biomicrofluidics*, 2011, **5,** 44107-441079.
12 S. Li et al., *Anal. Chem*., 2013, **85,** 5468-74.
13 F. A. A. Fergusson, E. W. Guptill, MacDonald, *J. Acoust. Soc. Am.,* 1954, **26,** 67.
14 C. J. Burton, *J. Acoust. Soc. Am.,* 1948, **20,** 186.

 This journal is © The Royal Society of Chemistry [year]